environmental microbiology

Environmental Microbiology (2022) **24**(9), 4411–4424 doi:10.1111/1462-2920.16039

Na^+ homeostasis in *Acinetobacter baumannii* is facilitated via the activity of the Mrp antiporter

Josephine Joy Hubloher, Lisa van der Sande and Volker Müller *

Department of Molecular Microbiology & Bioenergetics, Institute of Molecular Biosciences, Goethe-University Frankfurt am Main, Frankfurt, Germany.

Summary

The human opportunistic pathogen *Acinetobacter baumannii* is a global threat to healthcare institutions worldwide, since it developed very efficient strategies to evade host defence and to adapt to the different environmental conditions of the host. This work focused on the importance of Na^+ homeostasis in *A. baumannii* with regards to pathobiological aspects. *In silico* studies revealed a homologue of a multicomponent Na^+/H^+ antiporter system. Inactivation of the Mrp antiporter through deletion of the first gene (*mrpA′*) resulted in a mutant that was sensitive to increasing pH values. Furthermore, the strain was highly sensitive to increasing Na^+ and Li^+ concentrations. Increasing Na^+ sensitivity is thought to be responsible for growth impairment in human fluids. Furthermore, deletion of *mrpA′* is associated with energetic defects, inhibition of motility and survival under anoxic and dry conditions.

Introduction

The Gram-negative human pathogen *Acinetobacter baumannii* has become a threat for the global health care system since the early 1970s (Bergogne-Bérézin and Towner, 1996). Since then, the impact of *A. baumannii* on the global health care system is steadily increasing as well as the virulence potential and the multi-drug resistance profile of *A. baumannii* isolates (Poirel *et al*., 2003; Dijkshoorn *et al*., 2007; Falagas and Karveli, 2007; Peleg *et al*., 2012; Antunes *et al*., 2014; Jacobs *et al*., 2014). *Acinetobacter baumannii* is classified by the Infectious Diseases Society of America as one of the six most concerning multidrug-resistant nosocomial pathogens worldwide (Boucher *et al*., 2009; Antunes *et al*., 2014) and the World Health Organization published a list of concerning antibiotic-resistant 'priority pathogens' where carbapenem-resistant *A. baumannii* was grouped in the most critical category (World Health Organization, 2017).

The underlying molecular mechanisms that contribute to the fitness and success of *A. baumannii* in hospitals are more and more uncovered (McConnell *et al*., 2013; Harding *et al*., 2018; Morris *et al*., 2019). Plenty of different mechanisms – including adherence to biotic and abiotic surfaces, capsule assembly, desiccation resistance, nutrition acquisition and utilization, antibiotic resistance, and the ability to evade the immune systems are described to be crucial for the success of *A. baumannii* as a nosocomial pathogen (Lee *et al*., 2006; Antunes *et al*., 2011; Gebhardt *et al*., 2015; Stahl *et al*., 2015; Weidensdorfer *et al*., 2019; Zeilder and Müller, 2019a; Zeidler and Müller, 2019b, a; Chen, 2020; Hubloher *et al*., 2021; Talyansky *et al*., 2021). Furthermore, the ability to maintain ion homeostasis has been studied extensively in recent years. The role of potassium ions has been described to be crucial for *A. baumannii* pneumonia pathogenesis, resistance against reactive oxygen species and against antibacterial compounds (Samir *et al*., 2016; König *et al*., 2021). Additionally, the role of iron, manganese and zinc ions has been studied extensively (Hood *et al*., 2012; Mortensen and Skaar, 2013; Hesse *et al*., 2019; Runci *et al*., 2019; Green *et al*., 2020; Sheldon and Skaar, 2020). All these studies provide evidence that ion homeostasis is a crucial key factor for bacterial cell physiology and eventually for the success of *A. baumannii* in hospital settings.

This work aimed to highlight the role of sodium ions in the physiology of *A. baumannii*. Sodium ions are one of the most abundant ions in the human host reaching concentrations of 145 mM in human serum (McKee *et al*., 2016) and Na^+ concentrations up to a physiological maximum of 290 mM in human urine (Plough and Baker, 1959; Wang *et al*., 2013). High intracellular sodium ion concentrations are toxic for bacteria and therefore, the internal Na^+ concentrations need to be strictly regulated (Padan *et al*., 2005). On the other hand, sodium ions are essential for a plethora of different

Received 9 March, 2022; revised 26 April, 2022; accepted 4 May, 2022. *For correspondence. E-mail: vmueller@bio.uni-frankfurt.de; Tel. + 49 69 79829507; 49 69 79829306.

uptake or efflux processes where they are used as cosubstrate (Wilson and Ding, 2001). One fundamental challenge for bacteria is to maintain Na^+ and pH homeostasis. Therefore, bacteria usually encode multiple Na^+/H^+ antiporter (Hamamoto *et al*., 1994; Padan *et al*., 2005; Krulwich *et al*., 2009). Na^+/H^+ antiporter facilitate the efflux of sodium ions driven by the import of protons (Padan and Schuldiner, 1994). The transfer of protons is strictly coupled to pH homeostasis and results in an overlapping regulation of Na^+ and H^+ homeostasis (Padan *et al*., 2005; Krulwich *et al*., 2011). Most common Na^+/H^+ antiporter are single gene products; however, the so-called Mrp antiporter systems (also known as Sha/Mnh/Pha antiporters) are multicomponent systems (Padan *et al*., 2005; Ito *et al*., 2017). The Mrp antiporter is a hetero-oligomeric complex in the inner membrane of bacteria and consists of six to seven hydrophobic proteins (Ito *et al*., 2017). All proteins are usually required for full activity (Ito *et al*., 2017). Another outstanding property of the Mrp antiporter is that three proteins, MrpA, MrpD and MrpC, are similar to the membrane-spanning subunits of the NADH:ubiquinone oxidoreductase (complex I) NuoL, NuoM and NuoN (Berrisford *et al*., 2016; Ito *et al*., 2017; Steiner and Sazanov, 2020). Here, we studied the physiological role of the Mrp antiporter in *A. baumannii* ATCC 19606 and discovered that it is the major Na^+/H^+ exchange system in *A. baumannii* and is responsible for Na^+ and pH homeostasis.

Results

Putative Na^+ transporter genes in A. baumannii *ATCC 19606*

The genome of *A. baumannii* ATCC 19606 encodes for different Na^+ transport systems. Besides several unspecific putative outer membrane proteins (F911_00461, F911_00823, F911_00831, F911_00920, F911_01824, F911_01836, F911_02072, F911_02491, F911_02596, F911_02714, F911_02725, F911_03024, F911_03692) the genome of *A. baumannii* ATCC 19606 encodes a few genes annotated as putative Na^+ symporter, a predicted glutamate:Na^+-symporter (F911_01475), two Na^+:proline-symporter (F911_02201 and F911_00392), two bile acid:Na^+-symporter (F911_01887 and F911_00276), a Na^+(or H^+):dicarboxylate symporter (F911_02283), a Na^+:melibiose symporter (F911_02462) and a neurotransmitter: Na^+-symporter (F911_00236). In sharp contrast to other bacteria (Padan and Schuldiner, 1994), we only found two annotated putative Na^+/H^+ antiporter encoded in the genome of *A. baumannii* ATCC 19606. One is annotated as a putative single subunit Na^+/H^+ antiporter (F911_00974), but it is also similar to other monovalent or divalent cation antiporter such as the NhaP antiporter from *Pseudomonas aeruginosa* PAO1 (34% identity, 51% similarity). The second encodes subunits of a 'multiple resistance and pH regulation' antiporter, Mrp (F911_03564–F911_03569). The putative subunits are very similar to the proteins of group II Mrp antiporter (MrpA′CDEFG) (Fig. 1). In this group, the first two genes *mrpA* and *mrpB* are fused together to *mrpA′* (Ito *et al*., 2017). All genes of the putative *mrp* gene cluster encode for membrane proteins with predicted transmembrane helices ranging from 3 to 25 (supplement Table S1).

Markerless deletion of the mrpA′ *gene*

To study the role of the Mrp antiporter in the physiology of *A. baumannii* ATCC 19606 we decided to generate a deletion mutant. MrpA is essential for antiport function (Górecki *et al*., 2014; Ito *et al*., 2017) and thus, we deleted the *mrpA′* via an established insertion duplication system (Stahl *et al*., 2015). A scheme of the *mrp* gene cluster of the Δ*mrpA′* mutant is shown in the supplement Fig. S1. To this end, the flanking regions of the *mrpA′* gene were amplified and cloned in a vector that has a kanamycin-resistance marker. The plasmid was inserted via homologous recombination into the genome of *A. baumannii* ATCC 19606 and resulting integrants were subjected to sucrose-based counter-selection. Counter-selection should either restore the wild type locus or result in a markerless deletion of *mrpA′*. Theoretically, both events should happen with the same probability, but, after several tries, we were not able to identify a Δ*mrpA′* mutant using L0 medium (5 g L^{-1} yeast extract, 10 g L^{-1} tryptone) with 10% sucrose. In addition, all *mrp* genes are described to be potentially essential for growth of *A. baylyi* ADP1 in minimal medium (31 mM Na^+) with succinate as carbon and energy source (de Berardinis *et al*., 2008). We tried several conditions to obtain an *mrpA′* deletion mutant and addition of arabinose as carbon and energy source allowed to obtain the deletion mutant. Even though addition of arabinose seems to be crucial for deletion of *mrpA′* in the first place, the strain grew comparable to the wild type in L0 medium without any further sugars (Fig. 2A) and both strains reached a final optical density (OD_{600nm}) of ∼5 after approximately 4–5 h. Nevertheless, the growth rate of the wild type (1.4 h^{-1}) was slightly higher than the growth rate of the Δ*mrpA′* mutant (0.94 h^{-1}). In addition, colonies of the Δ*mrpA′* strain were smaller than wild type colonies on solid L0 medium (1.8% agar) (Fig. 2B). We assume that this may be due to a general energetic defect of the mutant (see below).

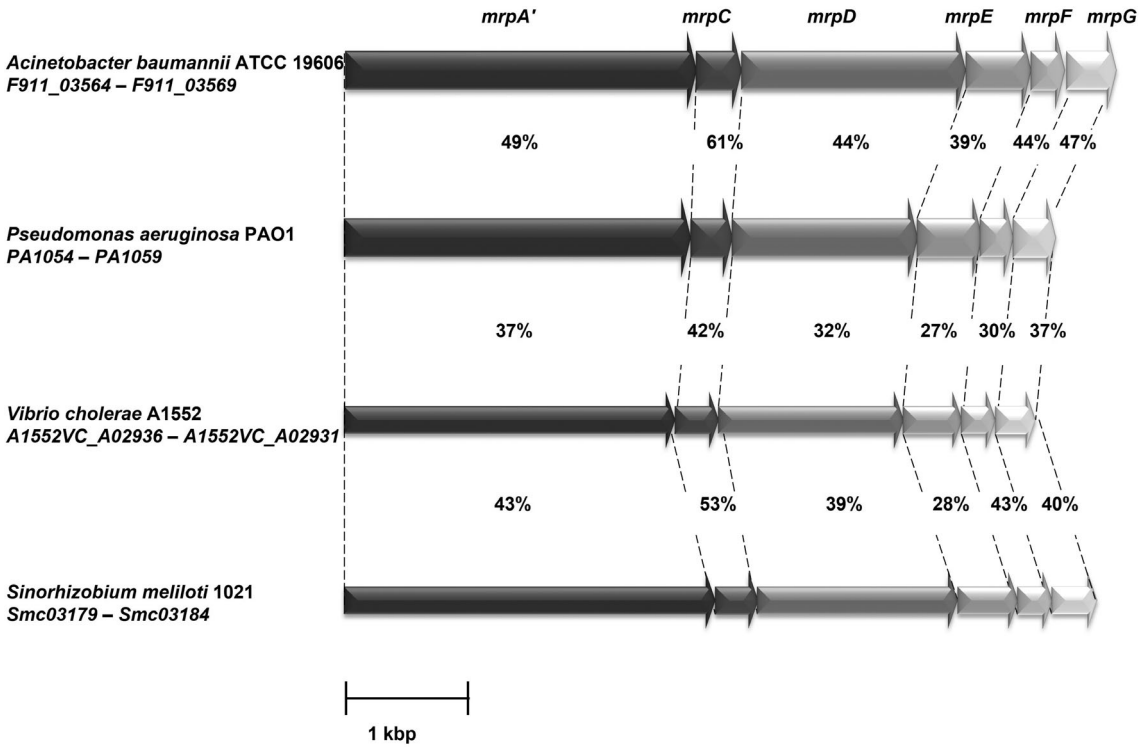

Fig. 1. Genetic organization of *mrp* gene cluster of *A. baumannii* and comparison to other Gram-negative bacteria. Identical subunits have the same lettering and numbers indicate the degree of identity.

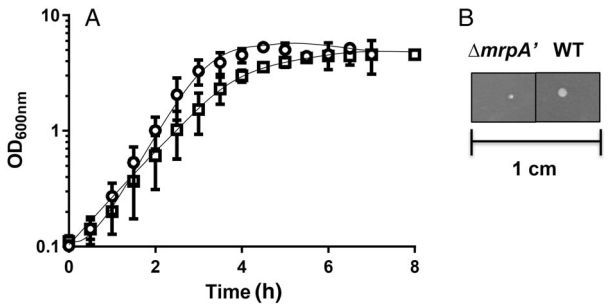

Fig. 2. Effect of deletion of *mrpA′* in *A. baumannii* ATCC 19606 on growth in L0 medium.
A. *Acinetobacter baumannii* ATCC 19606 (○) and Δ*mrpA′* (□) were grown in liquid L0 medium. Precultures were grown in L0 medium overnight and were used to inoculate prewarmed L0 medium to an initial OD_{600nm} of 0.1. Error bars denote the standard deviation calculated from at least three biological replicates.
B. Comparison of the colony size of *A. baumannii* ATCC 19606 and Δ*mrpA′* on solid (1.8% agar) L0 medium. One representative experiment is shown.

The Mrp antiporter activity is crucial for Na^+/Li^+ efflux in A. baumannii *ATCC 19606*

Na^+ and Li^+ are taken up by the earlier mentioned plethora of Na^+ transporter, but both are cytotoxic with Li^+ being more toxic than Na^+ (Inaba *et al*., 1994; Rimon *et al*., 2007). To address the role of the Mrp antiporter in Na^+ tolerance we grew *A. baumannii* ATCC 19606 and the Δ*mrpA′* mutant in L0 medium and added increasing amounts of NaCl (Fig. 3A and B). NaCl concentrations from 50 to 300 mM did not affect the growth of *A. baumannii* ATCC 19606. Growth of the wild type started immediately and proceeded with a growth rate between 1.5 and 1.3 h^{-1} (Fig. 3A). When no NaCl was added to the media growth of the Δ*mrpA′* mutant started immediately and proceeded with a growth rate of 0.97 h^{-1}. However, increasing NaCl concentrations resulted in an increasing growth inhibition of the Δ*mrpA′* mutant until growth was completely abolished in the presence of 200 and 300 mM NaCl (Fig. 3B).

Since Li^+ and Na^+ share a very similar radius Na^+-dependent enzymes can often use Li^+ instead of Na^+ (Boudker *et al*., 2007). To address the role of the Mrp antiporter in Li^+ tolerance we grew *A. baumannii* ATCC 19606 and the Δ*mrpA′* mutant in L0 medium with increasing LiCl concentrations (Fig. 3C and D). Growth of the wild type was not affected by addition of LiCl (≤50 mM) (Fig. 3C). In contrast deletion of the *mrpA′* gene resulted in a strong Li^+-dependent growth inhibition (Fig. 3D). The Δ*mrpA′* mutant did not grow in the presence of ≥5 mM LiCl. To verify that the growth inhibition is due to increasing Na^+/Li^+ concentrations, we repeated the experiment but added increasing KCl concentration (up to 300 mM) (Fig. 3E and F). Again, growth of the wild

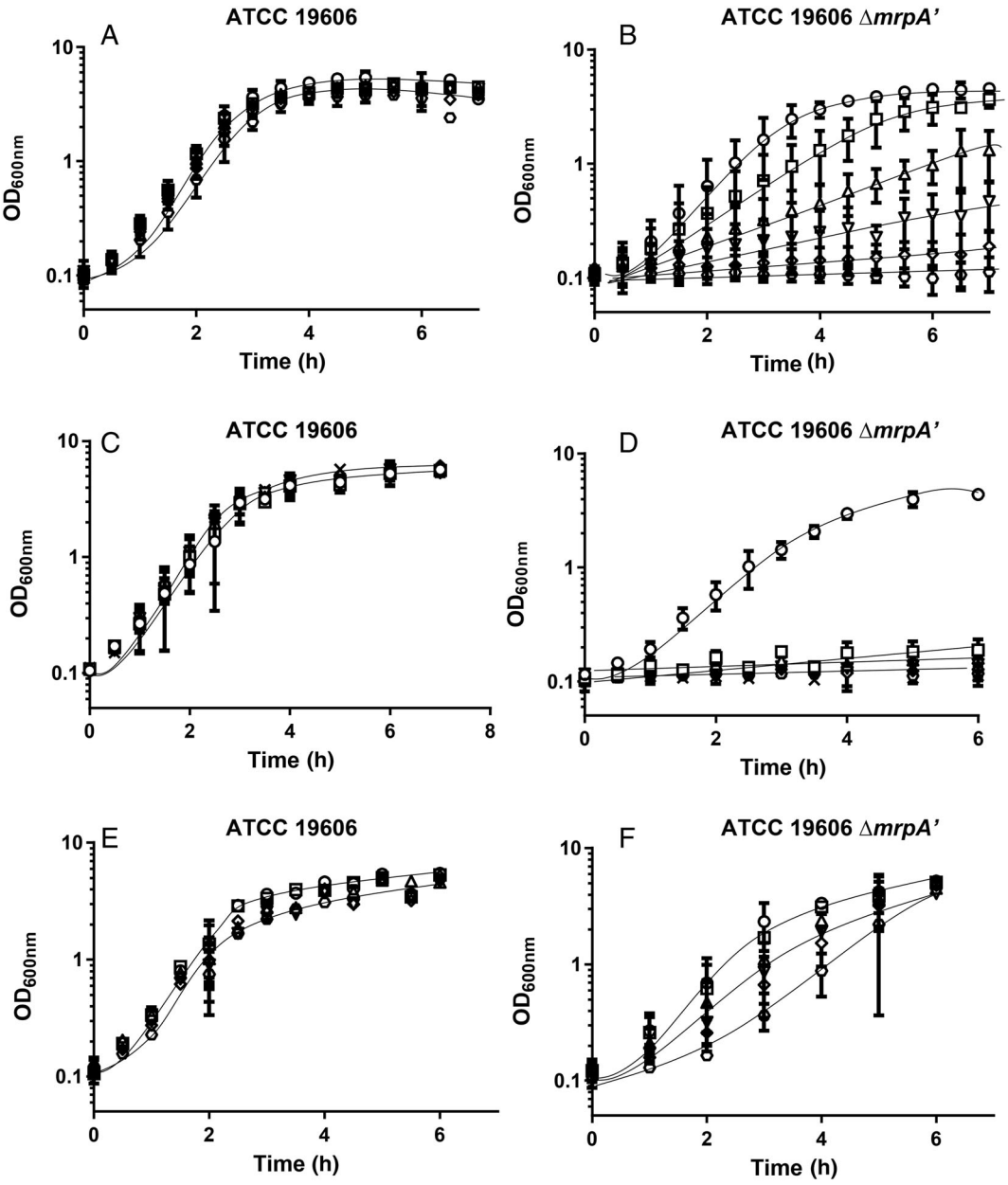

Fig. 3. Effect of deletion of *mrpA′* in *A. baumannii* ATCC 19606 on growth in L0 medium with increasing ion concentrations. *Acinetobacter baumannii* ATCC 19606 (A, C, E) and Δ*mrpA′* (B, D, F) were grown in L0 medium overnight. The precultures were used to inoculate prewarmed L0 medium to an initial OD_{600nm} of 0.1. (A + B) L0 medium contained increasing NaCl concentrations: 0 (◦), 50 (□), 100 (△), 150 (▽), 200 (◊) and 300 mM (⬡). (C + D) L0 medium contained increasing LiCl concentrations: 0 (◦), 5 (□), 10 (△), 20 (▽), 30 (◊) 40 mM (⬡) and 50 mM (x). (E + F) L0 medium contained increasing KCl concentrations: 0 (◦), 50 (□), 100 (△), 150 (▽), 200 (◊) and 300 mM (⬡). Error bars denote the standard deviation calculated from at least three biological replicates.

type was not affected by increasing KCl concentrations and growth of the *mrpA′* mutant was only marginally affected in presence of increasing KCl concentrations. This slight impairment of growth of the Δ*mrpA′* mutant may be caused by the high ionic strength. In sum, these studies are in accordance with the hypothesis that the Mrp antiporter is essential for Na^+ and Li^+ efflux in *A. baumannii*.

The Mrp antiporter of A. baumannii *ATCC 19606 is essential for adaptation to alkaline environments in a Na^+-dependent manner*

Besides their role in efflux of toxic Na^+ or Li^+, Mrp antiporter are known to be crucial for pH homeostasis and especially growth under alkaline conditions. To address the role of the Mrp in adaptation to high pH values we

grew *A. baumannii* ATCC 19606 and the Δ*mrpA′* mutant in L0 medium with adjusted initial pH values from 6 to 10 (Fig. 4). Growth of the wild type was only slightly affected by increasing pH values from 6 to 9. The external pH did not change significantly during growth. Growth proceeded with a growth rate of 1.5–1 h^{-1} (Fig. 4A). Only at pH 10 there was a lag phase of approximately 2 h and the growth rate was reduced to 0.7 h^{-1}. This pH sensitivity was even increased in the Δ*mrpA′* mutant. (Fig. 4B). Growth was strongly reduced at pH 9 and completely abolished at pH 10. The pH sensitivity of the Δ*mrpA′* mutant was even higher in media that contained Na^+ (Fig. 4C). Already low (50 mM) NaCl concentrations resulted in a dramatic growth impairment of the Δ*mrpA′* mutant with a growth rate of 0.31 h^{-1} at pH 8 and a complete growth inhibition at pH 9. In contrast, increasing NaCl concentrations did not – or only marginally – decrease the growth rate of the wild type at pH values of 8 or 9. Taken together, the Mrp antiporter of *A. baumannii* ATCC 19606 is essential for the adaptation to alkaline environments in a Na^+-dependent manner.

Complementation of the ΔmrpA′ *mutant in cis restored* Na^+ *and pH hypersensitivity*

To verify that the observed phenotypes were caused by the absence of *mrpA′* we performed complementation studies. Therefore, *mrpA′* was re-inserted into the genomic locus *F911_00233* of the Δ*mrpA′* mutant as described in Experimental procedures. We generated three strains – a complemented strain (Δ*mrpA′_F911_00233*::*mrpA′_kan*^{R}) and two control strains (Δ*mrpA′_F911_00233*::*kan*^{R} and ATCC 19606_*F911_00233*::*kan*^{R}) and analysed the growth under conditions that impaired growth of the Δ*mrpA′* mutant (5 mM LiCl, 300 mM NaCl and pH 10) (Fig. 3). All strains started to grow immediately in L0 medium with a growth rate of ∼1.1 h^{-1}. Growth of the ATCC 19606_*F911_00233*::*kan*^{R} strain was not inhibited by LiCl or NaCl. The increase of the pH value to 10 caused a prolonged lag phase of ∼2 h (supplement Fig. S2) as observed for the wild type (Fig. 4A). Growth of the Δ*mrpA′_F911_00233*::*kan*^{R} strain was impaired at pH 10 or in presence of LiCl/NaCl (supplement Fig. S2) as observed for the Δ*mrpA′* mutant. In contrast, growth inhibition at pH 10 or in presence of LiCl/NaCl was restored in the complemented strain (Δ*mrpA′_F911_00233*::*mrpA′_kan*^{R}) (supplement Fig. S2). These data provide evidence that growth impairment of the Δ*mrpA′* mutant is truly due to genetic inactivation of the Mrp antiporter.

The promoter of the mrp *gene cluster is constitutively active*

To analyse the effect of Na^+ and pH on expression of the *mrp* gene cluster we performed reporter gene assays. Therefore, the reporter gene *gusA* was fused to 700 bp upstream of the *mrpA′* gene in the plasmid pVRL2. *Acinetobacter baumannii* ATCC 19606 was transformed with the resulting reporter gene construct and grown in L0 medium at pH 7 with or without 200 mM NaCl or at pH 9 (Fig. 5A), sodium chloride was added in the exponential growth phase and the β-glucuronidase activity was measured over time (Fig. 5B). We observed a high activity of the β-glucuronidase in all experimental setups. Addition of NaCl or an increased pH did not result in a significant increase of the β-glucuronidase activity. For a better interpretation of the data we compared our results to a described reference. The MtlD promoter of *A. baumannii* ATCC 19606 was described to be only marginally expressed in mineral medium and induced by the addition of NaCl (Zeidler *et al.*, 2017). We cloned the

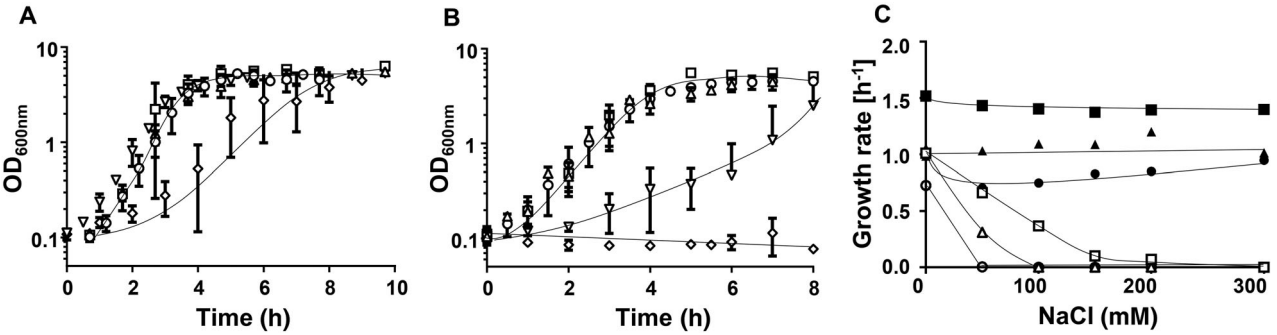

Fig. 4. Effect of deletion of *mrpA′* in *A. baumannii* ATCC 19606 on growth in L0 medium with increasing pH values. *Acinetobacter baumannii* ATCC 19606 (A) and Δ*mrpA′* (B) were grown in L0 medium with increasing pH values. Precultures were grown in L0 medium (pH 7) overnight and were used to inoculate prewarmed medium to an initial OD_{600nm} of 0.1 with adjusted inital pH values of 6 (○), 7 (□), 8 (△), 9 (▽) or 10 (◇). Error bars denote the standard deviation from at least three biological replicates. (C) Growth rate of *A. baumannii* ATCC 19606 (closed symbols) and Δ*mrpA′* (open symbols) calculated from grown cells in L0 medium with adjusted initial pH values of 7 (□), 8 (△) or 9 (○) and indicated NaCl concentrations.

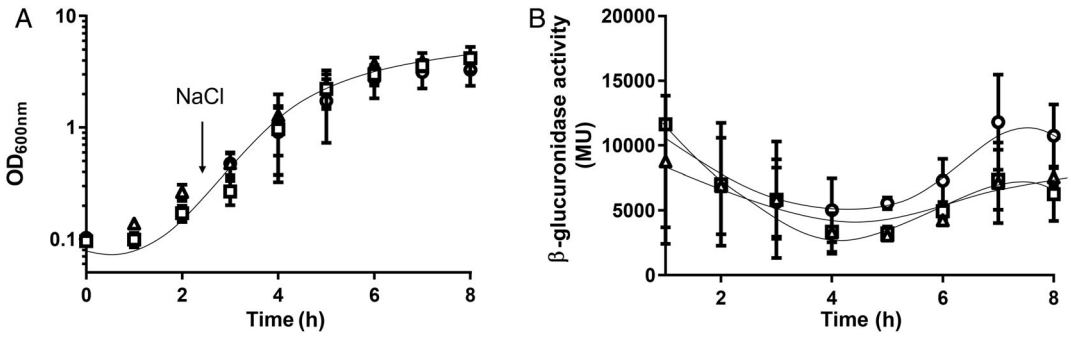

Fig. 5. Promoter activity of the *mrp* gene cluster as determined by reporter gene assays.
A. Growth and (B) corresponding β-glucuronidase activity of the reporter gene strain ATCC 19606 + pVRL2_up_*mrpA′_gusA* grown in L0 medium (△) with 200 mM NaCl (○) or at pH 9 (□) in presence of 100 μg ml^{-1} gentamicin. Error bars denote standard deviation calculated from at least three biological replicates.

upstream region of the *mtlD* gene in front of the reporter gene and analysed the promoter activity (for full data set see supplement Fig. S3). In the absence of NaCl the activity of the β-glucuronidase was very low [approximately 500 (MU)], but addition of NaCl increased β-glucuronidase activity to 8000 (MU) (Fig. S3). In comparison in the *mrp* reporter gene strain the β-glucuronidase activities varied between 5000 and 10 000 (MU). These data provide evidence that Na^+ and pH do not specifically induce expression of the *mrp* gene cluster, which is already expressed at a high level.

The Mrp antiporter is involved in ATP homeostasis in A. baumannii *ATCC 19606*

Since the Δ*mrpA′* colonies were smaller than the wild type colonies we asked whether the Mrp antiporter has a role in energy homeostasis. To address the role of the Mrp antiporter in cellular ATP homeostasis we measured the ability of wild type and the Δ*mrpA′* mutant to generate and maintain ATP. ATP synthesis was induced after addition of tryptone and the ATP level was monitored over a time course of 18 h (Fig. 6). The wild type and the Δ*mrpA′* mutant started to accumulate ATP after addition of tryptone with a maximum after 2 h. The maximum ATP yields of the wild type and the Δ*mrpA′* mutant were comparable. Thereafter, the ATP concentration decreased over time. This holds true for both strains; however, the ATP pool decreased more rapidly in the Δ*mrpA′* mutant. After 8 h, the ATP concentration was reduced to 1.8 ± 0.2 nmol ATP mg^{-1} protein in the wild type but to approximately half (0.8 ± 0.1 nmol ATP mg^{-1} protein) in the mutant. After 6 more hours the wild type cells reached a comparable drop of the ATP pool with 0.7 ± 0.2 nmol ATP mg^{-1} protein. These data provide evidence that deletion of *mrpA′* of *A. baumannii* ATCC 19606 resulted in a mutant that is impaired in ATP maintenance.

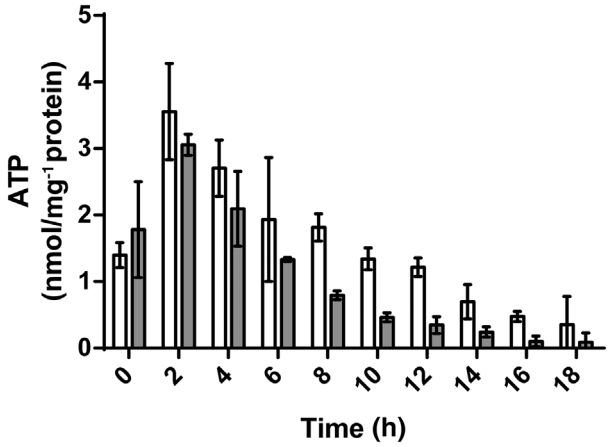

Fig. 6. Intracellular ATP levels in *A. baumannii* ATCC 19606 and the Δ*mrpA′* mutant. *Acinetobacter baumannii* ATCC 19606 (white bars) and Δ*mrpA′* (grey bars) were grown overnight in L0 medium, and cell suspensions were prepared. ATP synthesis was induced by addition of tryptone. The intracellular ATP content was quantified as described in Experimental procedures. Error bars denote the standard deviation calculated from at least three biological replicates.

Role of Mrp in energy-consuming processes

Acinetobacter baumannii can spread over surfaces by twitching motility and can survive under strictly anoxic conditions in the human gut or on dry surfaces within the hospital. Both processes are energy (ATP-) dependent. To analyse the physiological role of the Mrp antiporter on motility of *A. baumannii* we generated an AYE-T Δ*mrpA′* strain. We used the AYE-T strain (Godeux *et al*., 2020) as parental strain since the strain ATCC 19606 is unable to move across surfaces (Grier *et al*., 2021). Deletion of *mrpA′* from strain AYE-T was difficult and only possible in mineral medium with succinate as carbon source. Furthermore, the *mrpA′* mutant was impaired in growth in complex medium (L0 medium or tryptone medium) (data not shown). Growth impairment could be overcome by addition of arabinose (data not shown), indicating an

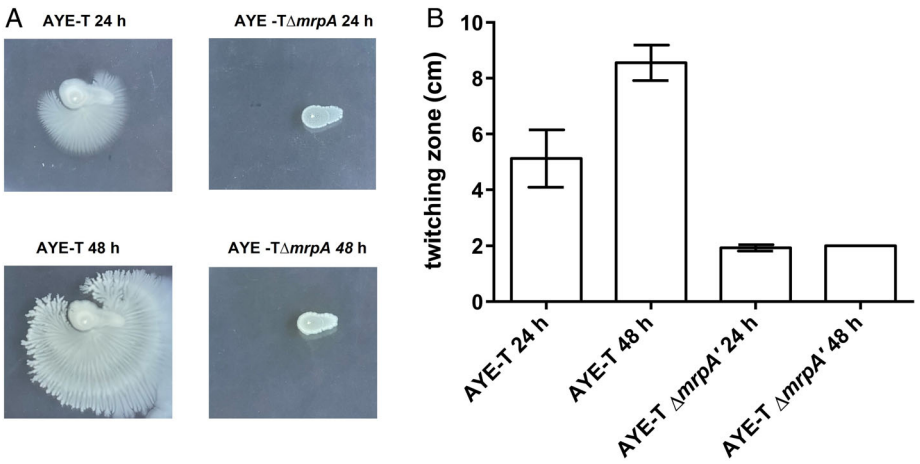

Fig. 7. Twitching motility *of A. baumannii* strain AYE-T and Δ*mrpA′*. 5 µl of an overnight culture of *A. baumannii* AYE-T and Δ*mrpA′* were spotted on a semi-solid motility plate.
A. Representative twitching on motility plates.
B. Average diameter of twitching zone from *A. baumannii* AYE-T and Δ*mrpA′*. Error bars denote the standard deviation calculated from at least three biological replicates.

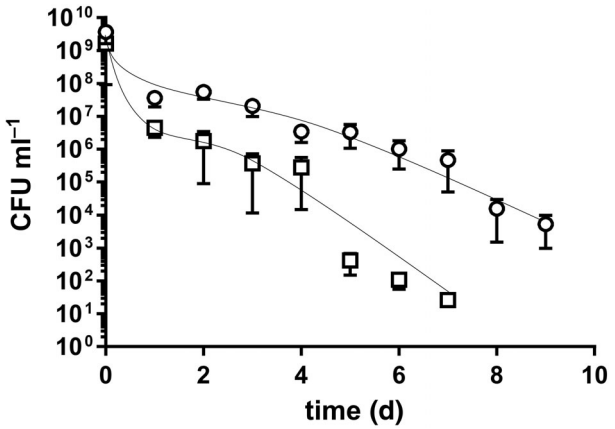

Fig. 8. Survival of *A. baumannii* ATCC 19606 wild type and Δ*mrpA′* under anoxic conditions. 50 ml anoxic L0 medium was inoculated with *A. baumannii* wild type or Δ*mrpA′* overnight cultures and incubated at 37°C and 130 rpm. Cell survival was monitored by determining the CFU ml^{-1}. Error bars denote the standard deviation calculated from at least three biological replicates.

energetic defect of the AYE-T Δ*mrpA′* mutant. Then, we analysed twitching motility of the AYE-T strains on motility plates in the presence of arabinose (0.5% tryptone, 20 mM arabinose and 0.3% agarose). As can be seen in Fig. 7 the ability of the AYE-T strain to twitch across surfaces was completely abolished by deletion of *mrpA′* (Fig. 7).

Survival of a strict aerob like *A. baumannii* requires the maintenance of a membrane potential, likely by K^+ export or H^+ export driven by ATP hydrolysis. Therefore, we checked for survival of *A. baumannii* ATCC 19606 and Δ*mrpA′* under strictly anoxic conditions (Fig. 8). To our surprise, the strict aerob survived for a long time. After 9 days, still $\sim 1 \times 10^4$ CFUs ml^{-1} were present. In contrast the tolerance to strictly anoxic conditions was three orders of magnitude lower in the Δ*mrpA′* mutant.

The Mrp antiporter of A. baumannii *ATCC 19606 is essential for growth in Na^+ rich human liquids and for desiccation resistance*

One of the major factors for *A. baumannii's* success to conquer the hospital environment is its desiccation resistance. Survival under dry conditions was also affected in the ATCC 19606 Δ*mrpA′* mutant. As can be seen in Fig. 9, the Δ*mrpA′* mutant was highly sensitive to desiccation in comparison to the wild type. Whereas $\sim 1 \times 10^6$ CFU ml^{-1} survived in the wild type after 5 days of desiccation the Δ*mrpA′* cells completely lost viability. The decreased desiccation resistant of the mutant *mrpA′* was restored by complementation (supplement Fig. S4).

Acinetobacter baumannii ATCC 19606 can grow in human urine (Fig. 10), as shown before (Di Venanzio *et al*., 2019; Hubloher *et al*., 2021), but growth of the Δ*mrpA′* mutant was largely impaired (Fig. 10). Complementation of the Δ*mrpA′* mutant restored growth in human urine (data not shown). A similar observation was made for growth in heat-inactivated human serum (supplement Fig. S5). We inoculated 5 ml of inactivated human serum to an initial optical density of 0.1. After 24 h of incubation the wild type reached an OD_{600nm} of 0.75 ± 0.05, whereas the Δ*mrpA′* mutant did not grow ($OD_{600nm} = 0.16 \pm 0.04$) (supplement Fig. S5). This phenotype was restored by complementation (supplement Fig. S5). A closer examination showed that the Δ*mrpA′* mutant is not only impaired in growth but instead the Δ*mrpA′* mutant is fastly inactivated, presumably due to intracellular Na^+ toxification (Fig. 10). In addition, the promoter activity of the *mrp* gene cluster during growth in human liquid was quite high demonstrating that the *mrp* gene cluster is expressed during growth in human liquids (Fig. 10). These data provide evidence that the Mrp antiporter activity is important for the adaptation to Na^+ rich host conditions.

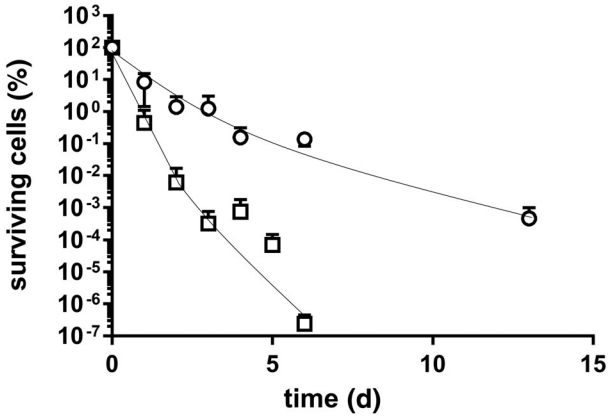

Fig. 9. Desiccation resistance of *A. baumannii* ATCC 19606 and Δ*mrpA′*. *Acinetobacter baumannii* strains were spotted on culture plates and incubated in a climate chamber at 22°C and 31% RH. Bacteria were removed from the plates by re-suspending with 360 µl K^+ phosphate buffer (10 mM, pH 6.8). Appropriate dilutions were prepared and cell forming units were determined on solid L0 medium. Error bars denote the standard deviation calculated from at least three biological replicates.

Discussion

Intracellular Na^+ homeostasis is crucial for bacteria to maintain physiological processes. Bacteria couple H^+ or Na^+ circulation to generate driving forces for uptake or efflux of substrates or ions and to maintain physiological cytoplasmic ion concentrations (Mitchell, 1961; Skulachev, 1991). Most bacteria generate a primary H^+ gradient (Mitchell, 1961) by primary H^+ pumps (e.g. respiratory ion pumps) that is then used by proton motive force ($\tilde{\mu}_{H+}$) -consuming processes (e.g. H^+-dependent ATP synthases, motility, solute transport or reverse electron transport) (Mitchell, 1961; Skulachev, 1991; Müller and Hess, 2017). Some bacteria especially anaerobic and marine bacteria also have primary Na^+ pumps such as dicarboxylate decarboxylase, methyltransferase, NQR complex that generate a primary Na^+ potential across the cytoplasmic membrane that then drives energy-consuming processes such as ATP synthesis, substrate uptake, motility and efflux of antibiotics (Dimroth, 1980; Skulachev, 1989; Heise *et al*., 1992; Müller and Gottschalk, 1992; Müller and Bowien, 1995; Schuchmann and Müller, 2014; Steuber *et al*., 2014; Ito *et al*., 2017; Müller and Hess, 2017; Kremp and Müller, 2020). The genome of *A. baumannii* does not encode a primary Na^+ pump such as the NQR complex. However, Na^+ is cytotoxic and bacteria need to maintain low internal Na^+ concentrations as well as a Na^+ gradient across their membranes to drive solute transport and motility (Padan and Schuldiner, 1993). This is achieved by Na^+/H^+ antiporter (Padan and Schuldiner, 1994; Farwick *et al*., 1995; Perez *et al*., 2014). In addition every living cell employs Na^+/H^+ antiport for Na^+ homeostasis and pH regulation. As we report here, *A. baumannii* is capable to couple Na^+ efflux with H^+ influx via the Mrp antiporter. Most neutrophilic bacteria are capable to grow in a rather broad pH range usually between 5.5 and 9 (Booth, 1985). The same seems to be true for *A. baumannii* as reported here. To guarantee an internal pH that maintain enzymatic functions bacteria adjust their internal pH in a narrow range of 7.4–7.8 (Padan *et al*., 2005). Therefore, under alkaline external conditions bacteria actively acidify their cytoplasm via Na^+/H^+ antiporter by H^+ uptake coupled to Na^+ export (Hamamoto *et al*., 1994; Kosono *et al*., 1999; Padan *et al*., 2005; Schubiger *et al*., 2020). Thereby, two birds are killed with one stone: pH regulation and generation of a sodium motive force. As we describe here MrpA′ of *A. baumannii* is essential pH regulation as well as Na^+, Li^+-dependent manner export.

As reported for other Mrp antiporter (e.g. *Bacillus* and *Dietzia*) (Ito *et al*., 1999; Kosono *et al*., 1999; Ito *et al*., 2000; Fang *et al*., 2018) Na^+ efflux in an Na^+ rich complex medium is facilitated by the Mrp antiporter in *A. baumannii*. Na^+ is omnipresent in the human host with Na^+ concentrations above 50 mM within human liquids [e.g. in urine and blood serum (Plough and Baker, 1959; Wang *et al*., 2013; McKee *et al*., 2016)]. Therefore, Na^+ cycling is discussed to be crucial for bacteria during infection of the human host (Dibrov *et al*., 2004). Consequently, the dependence on the Mrp antiporter during growth in human liquids shows that *A. baumannii* relies on Mrp-dependent Na^+ cycling. This is in line with the observation of decreased virulence of *mrp* mutants of *Pseudomonas aeruginosa* and *Staphylococcus aureus* in a mice infection model (Kosono *et al*., 2005; Vaish *et al*., 2018). The reduced ability of the *P. aeruginosa mrp* mutant to colonize and infect mice is thought to be due to Na^+-dependent impairments in host adaptation (Kosono *et al*., 2005).

We assume that inactivation of the Mrp antiporter in *A. baumannii* causes alterations in Na^+ cycling and may also cause interferences with H^+ cycling. This disorder in H^+ cycling might cause alterations in ATP homeostasis and subsequently impairments in ATP-dependent processes like motility and long-term survival. Another explanation for the observed phenotypes might be a continuous Na^+ influx resulting in a self-detoxification over time that causes depletion of the cellular ATP content, motility inhibition and decreased viability. This pleiotropic has been reported before in an *mrp* mutant of *P. aeruginosa* that is also unable to move across surfaces (Schubiger *et al*., 2020).

Our data fit well with the current knowledge about Mrp-dependent Na^+ and H^+ homeostasis and we provide evidence that Na^+ cycling is crucial for adaption of *A. baumannii* to the human host. We assume that *A.*

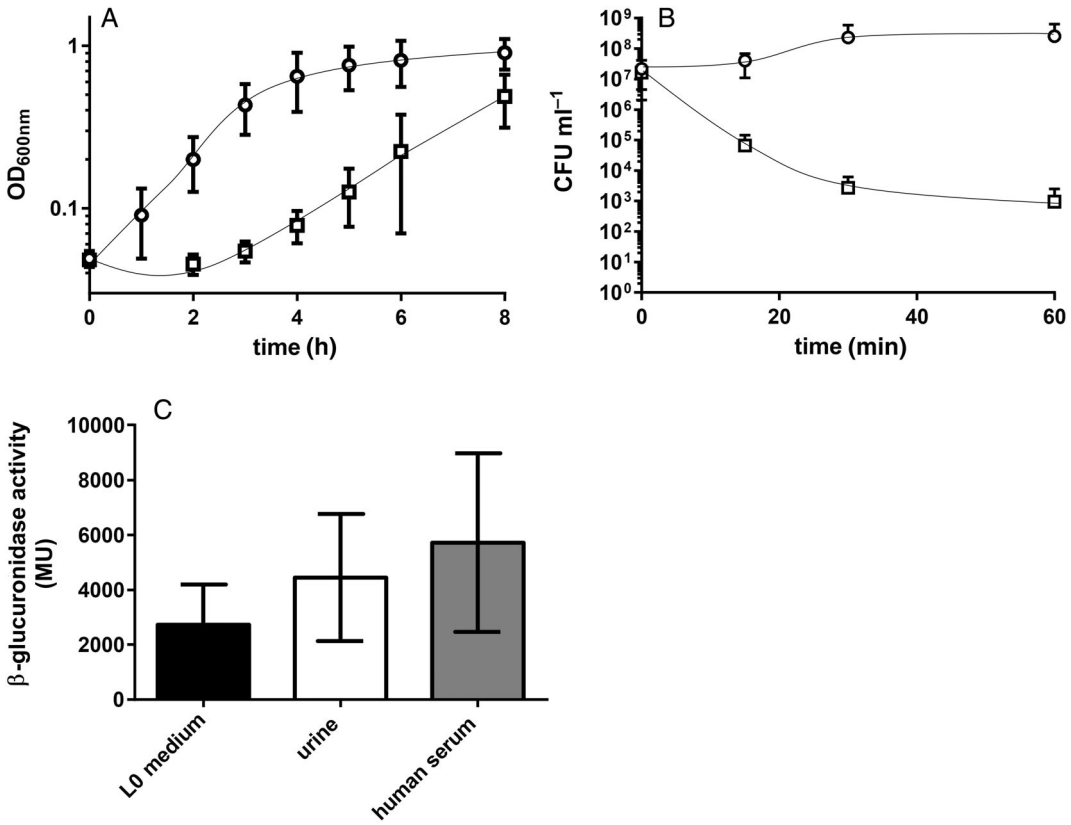

Fig. 10. Growth and survival of *A. baumannii* wild type and Δ*mrpA′* in human liquids.A.
Acinetobacter baumannii wild type (◦) and Δ*mrpA′* (□) were grown in L0 medium overnight and washed twice in K^+ phosphate buffer (10 mM, pH 6.8) before inoculation of fresh prewarmed human urine. Error bars denote the standard deviation from at least three biological replicates.
B. Survival of *A. baumannii* wild type (◦) and Δ*mrpA′* (□) in inactivated human serum. Strains were grown overnight in L0 medium and were incubated with heat-inactivated human serum at 37°C for 1 h. At designated timepoints CFUs were determined on solid L0 medium. Error bars denote the standard deviation from at least three biological replicates.
C. Promoter activity of the *mrp* gene cluster as determined by reporter gene assays. The reporter gene strain ATCC 19606 - + pVRL2_up_*mrpA′_gusA* was grown in L0 medium, human urine or in heat-inactivated human serum for 6 h in presence of 100 μg ml^{-1} gentamicin. The β-glucuronidase activity was determined. Error bars denote standard deviation calculated from at least three biological replicates.

baumannii uses Na^+ as coupling ion for substrate uptake during infection and consequently Na^+ efflux is essential for efficient cell growth during infection. Moreover, we assume that the Mrp antiporter might be essential to generate the SMF in the first place and second in pH regulation under alkaline conditions.

Experimental procedures

Bacterial strains

Escherichia coli DH5α was used for generation of recombinant plasmids. *Acinetobacter baumannii* strains ATCC 19606 and AYE-T (Godeux *et al*., 2020) were used as wild type strains. For growth of the strains LB medium (5 g L^{-1} yeast extract, 10 g L^{-1} tryptone, 5 g L^{-1} NaCl; pH 7), L0 medium (5 g L^{-1} yeast extract, 10 g L^{-1} tryptone; pH 7) or mineral medium [consisted of 50 mM K^+ phosphate buffer, pH 6.8; mineral solution (Zeidler *et al*., 2017) and 20 mM succinate] was used. The Na^+ concentration of the L0 medium determined *via* a Na^+ electrode was ∼8 mM. Growth experiments were performed in flasks with 100 ml cell culture at 37°C and 130 rpm. Salts (NaCl, LiCl or KCl) were added individually as indicated and if necessary, the initial pH was adjusted by the addition of KOH or HCl. Growth experiments were started by inoculation of prewarmed medium to an initial optical density at 600 nm (OD_{600nm}) of 0.1 and growth was monitored photometrically by measuring the OD_{600nm}.

Markerless deletion of mrpA′ *in* A. baumannii *ATCC 19606*

Markerless deletion of *mrpA′* (*F911_03564*) in *A. baumannii* ATCC 19606 was achieved via the *sacB*-based insertion–duplication system as described before (Stahl *et al*., 2015). Briefly, 1500 bp up- and downstream

of the *mrpA′* gene were amplified via PCR. The up- and downstream regions were cloned into pBIISK_*sacB_kanR* vector using Gibson assembly, according to the instructions of the manufacturer (Gibson Assembly Master Mix, New England Biolabs, Ipswich, MA, USA) (primers used are listed in the supporting information Table S2). The generated plasmids pBIISK_*sacB_kan*^{R}_Δ*mrpA′* were transformed in *A. baumannii* ATCC 19606 via electroporation (2.5 kV, 200 Ω and 25 μF). Resulting integrants were selected on LB medium with 1.8% agar and 50 μg ml^{-1} kanamycin. Counterselection was applied by the addition of 10% sucrose to L0 medium supplemented with 20 mM arabinose. Deletion of the *mrpA′* gene was verified via PCR.

RecAB-mediated deletion of mrpA′ *in* A. baumannii *AYE-T*

Deletion of *mrpA′* in *A. baumannii* AYE-T was done by recombineering (Tucker *et al*., 2014). 300 bp up- und downstream of the *mrpA′* gene were amplified from genomic DNA of *A. baumannii* AYE-T. A kanamycin-resistance marker was amplified from the plasmid pDK4 and the vector pBIISK was used as backbone (all primers used are listed in Table S2). The resulting PCR products were assembled using 'Gibson assembly' according to the instructions of the manufacturer (Gibson Assembly Master Mix, New England Biolabs) resulting in the plasmid pBIISK_Δ*mrpA′*::*kan*^{R}. A linear PCR fragment was amplified from the plasmid (primers are listed in Table S2). The resulting PCR was used for recombineering (Tucker *et al*., 2014). Briefly, *A. baumannii* ATCC 19606 + pAT04 was transformed with the PCR product according to the recombineering instructions (Tucker *et al*., 2014) and *A. baumannii* ATCC 19606 Δ*mrpA′*::*kan*^{R} was selected on solid (1.8% agar) mineral medium containing 20 mM succinate and 15 μg ml^{-1} kanamycin. The genetic exchange was verified by PCR. The kanamycin cassette was removed from the genome via the flippase-based deletion according to the recombineering protocol (Tucker *et al*., 2014) and resulted in a markerless deletion of *mrpA′* in the *A. baumannii* strain AYE-T.

Construction of the inserts for RecAB-mediated gene insertion

Genetic complementation of the ATCC 19606 Δ*mrpA′* mutant was done by insertion of *mrpA′* into the genomic locus *F911_00233* of *A. baumannii* ATCC 19606 Δ*mrpA′*. In addition, a kanamycin cassette was integrated into the genomic locus *F911_00233* of *A. baumannii* ATCC 19606 wild type and the Δ*mrpA′* mutant. Genetic insertion was mediated via the RecAB-recombineering system (Tucker *et al*., 2014) as described elsewhere (Hubloher *et al*., 2020).

Briefly, two recombinant plasmids pBIISK_*mrpA′*_complementation and pBIISK_*kan*^{R} were generated. We amplified the *mrpA′* coding sequence and the upstream region of *mrpA′* from genomic DNA of *A. baumannii* 19606 via PCR. A kanamycin resistance marker was amplified from the pDK4 and 300 bp flanking the insertion site (genomic locus *F911_00233*) were amplified from the genomic DNA of *A. baumannii* ATCC 19606. The vector pBIISK was used as backbone (all primers used are listed in Table S2). The resulting PCR products were assembled using 'Gibson assembly' according to the instruction of the manufacturer (Gibson Assembly Master Mix, New England Biolabs), resulting in the plasmid pBIISK_*mrpA′*_complementation.

To generate the plasmid pBIISK_*kan*^{R}, we amplified a kanamycin-resistance marker from pKD4 and 300 bp flanking the insertion site (genomic locus *F911_00233*) from genomic DNA of *A. baumannii* ATCC 19606. The vector pBIISK was used as backbone (all primers used are listed in Table S2). The resulting PCR products were assembled using 'Gibson assembly' according to the instruction of the manufacturer (Gibson Assembly Master Mix, New England Biolabs), resulting in the plasmid pBIISK_*kan*^{R}. The two recombinant plasmids pBIISK_*mrpA′*_complementation and pBIISK_*kanR* were amplified via PCR (primers used are listed in Table S2) and the PCR products were integrated into the genome as described below.

RecAB-mediated recombineering for gene insertion

Complementation of the mutant was done by recombineering as described before with slight modifications (Tucker *et al*., 2014; Hubloher *et al*., 2020). The RecAB producing strains *A. baumannii* ATCC 19606 + pAT04 and *A. baumannii* ATCC 19606 Δ*mrpA′* + pAT04 were transformed via electroporation (2.5 kV, 200 Ω and 25 μF) with 5 μg of the PCR products as described (Tucker *et al*., 2014), followed by selection on L0-medium (1.8% agar) containing kanamycin (7.5, 10 or 15 μg ml^{-1}). Thereby, we generated three strains: a complemented strain (Δ*mrpA′_F911_00233*::*mrpA′_kan*^{R}) and two control strains (Δ*mrpA′_F911_00233*::*kan*^{R} and ATCC 19606_*F911_00233*::*kan*^{R}). The genotype of the strains was verified using PCR.

Reporter gene studies

To analyse the promoter activity of the *mrp* gene cluster we performed reporter gene assays. Therefore, we amplified the upstream region of *mrpA′* (700 bp) from genomic DNA of *A. baumannii* ATCC 19606 and the reporter gene

gusA from the plasmid pIM1440 (Murin *et al*., 2012). The vector pVRL2 (Lucidi *et al*., 2018) was used as backbone (all primers used are listed in Table S2). The resulting PCR products were assembled using 'Gibson assembly' according to the instruction of the manufacturer (Gibson Assembly Master Mix, New England Biolabs) resulting in the construct pVRL2_*upmrpA′_gusA*. For generation of the *mtlD* reporter gene construct we exchanged the *mrpA′* upstream region against the *mtlD* upstream region. Therefore, the reporter gene construct was amplified omitting the *mrpA′* upstream region. The upstream region of *mtlD* was amplified from genomic DNA of *A. baumannii* ATCC 19606 (primers are listed in Table S2). The PCR products were assembled using 'Gibson assembly' according to the instruction of the manufacturer (Gibson Assembly Master Mix, New England Biolabs).

Acinetobacter baumannii ATCC 19606 was transformed with the reporter gene constructs via electroporation (2.5 kV, 200 Ω and 25 μF) and transformants were selected on solid LB-medium (1.8% agar) containing gentamicin (100 μg ml^{-1}). To analyse the pH-dependent promoter activity *A. baumannii* ATCC 19606 + pVRL2_*upmrpA′_gusA* was grown in L0 medium at pH 7 or 9. To analyse the Na^+-dependent promoter activity *A. baumannii* ATCC 19606 + pVRL2_*upmrpA′_gusA* was grown in L0 medium at pH 7 and 200 mM NaCl was added in the exponential growth phase. At defined time points the β-glucuronidase activity was measured as described previously (Zeidler *et al*., 2017).

Determination of the cellular ATP concentration

Acinetobacter baumannii ATCC 19606 and Δ*mrpA′* were grown overnight in L0 medium, harvested (4700 rpm, 30 min 4°C), cells were washed in 50 mM Tris–HCl buffer (pH 7.5) and afterwards re-suspended in Tris buffer (50 mM pH 7.5). The protein concentration of the cell suspension was quantified according to Schmidt *et al*. (1963) and adjusted to 1 mg ml^{-1}. The cell suspension was incubated at 37°C and ATP synthesis was induced by addition of tryptone (5 g L^{-1}). Samples were taken as indicated. 400 μl of the cell suspension was mixed with 150 μl perchloric acid (3 M, precooled on ice), followed by incubation on ice (5 min). The samples were neutralized by addition of 40 μl saturated K_2CO_3 solution and 80 μl TES buffer (400 mM, pH 7.6). After neutralization, the samples were centrifugated (3 min, 4°C, 14 400 rpm) and the supernatant was frozen in liquid nitrogen and stored overnight at −80°C. The ATP content of the samples was measured the next day using the ATP Bioluminescence Assay kit CLS II from Roche. 100 μl of the ATP containing sample was mixed with 20 μl of the luciferase containing solution and the ATP-dependent light emission was measured at the entire spectra in a microplate reader (Fluo star omega). An ATP calibration curve (0–500 pmol/assay) was used for quantification.

Desiccation assay

Desiccation assays were performed as described earlier with slight modifications (Zeidler and Müller, 2019b). Bacteria were grown overnight in 5 ml L0 medium, harvested, washed twice in H_2O and adjusted to an initial OD_{600nm} of 2. Aliquots of 40 μl were spotted on cell culture plates [12-well Nunclon Delta surface plate from Thermo scientific (Waltham, MA, USA)] and incubated in a climate chamber at 22°C and 31% relative humidity (RH). Bacteria were re-suspended in 360 μl K^+ phosphate buffer (10 mM, pH 6.8). Appropriate dilutions were prepared and colony-forming units were determined on solid L0 medium.

Growth in human urine

Growth studies in human urine were performed as described (Hubloher *et al*., 2021) with slight modifications. Briefly, cells were grown overnight in L0 medium, harvested by centrifugation (4700 rpm, 5 min), washed and re-suspended in sterile K^+ phosphate buffer (10 mM, pH 6.8). The cell suspensions were used to inoculate prewarmed urine (50 ml) to an initial OD_{600nm} of 0.05. Cells were grown at 37°C and 130 rpm, and growth was monitored photometrically by measuring the optical density at 600_{nm}.

Growth of A. baumannii *in inactivated human serum*

Acinetobacter baumannii strains were grown overnight in L0 medium. 5 ml heat-inactivated human serum [Sigma Aldrich (St. Louis, MO, USA)] was inoculated to an initial $OD600_{nm}$ of 0.1 and incubated at 37°C and 130 rpm for 24 h. Appropriate dilutions were prepared in inactivated human serum and the OD_{600nm} was measured photometrically.

Survival of A. baumannii *in human serum*

For determination of cell survival, cells were grown overnight in L0 medium and washed twice in K^+ phosphate buffer (10 mM, pH 6.8). Inactivated human serum (100%) was inoculated with bacteria to an initial CFU ml^{-1} of approximately 1×10^7. The bacteria-serum suspension was incubated at 37°C and CFU ml^{-1} was determined on solid L0 medium.

Twitching motility

Acinetobacter baumannii AYE-T and Δ*mrpA′* were grown for 8 h in liquid mineral medium with 20 mM succinate as carbon source. 5 µl of the culture was placed on top of a semi-solid motility plate (0.5% tryptone, 20 mM arabinose and 0.3% agarose). Bacteria were allowed to move across the semisolid agarose surface at 37°C. The twitching zone was documented and measured after 24 and 48 h.

Survival of A. baumannii *under anoxygenic conditions*

120 ml serum bottles were filled with 50 ml L0 medium. The medium was sparged with N_2 (100%) for 20 min and an N_2-atmosphere was applied. The anoxic medium was inoculated with 5 ml of an *A. baumannii* overnight culture grown in L0 medium via injection. Followed by incubation at 37°C and 130 rpm. Samples were taken, appropriate dilutions were prepared and cell forming units were determined on solid L0 medium.

Acknowledgements

The authors are indebted to the Deutsche Forschungsgemeinschaft for financial support via DFG Research Unit FOR 2251. *Acinetobacter baumannii* strain AYE-T was kindly provided by Prof. Xavier Charpentier from the Claude Bernard University, Lyon, France.

References

Antunes, L.C.S., Imperi, F., Carattoli, A., and Visca, P. (2011) Deciphering the multifactorial nature of *Acinetobacter baumannii* pathogenicity. *PLoS One* **6**: e22674.

Antunes, L.C.S., Visca, P., and Towner, K.J. (2014) *Acinetobacter baumannii*: evolution of a global pathogen. *Pathog Dis* **71**: 292–301.

Bergogne-Bérézin, E., and Towner, K.J. (1996) *Acinetobacter* spp. as nosocomial pathogens: microbiological, clinical, and epidemiological features. *Clin Microbiol Rev* **9**: 148–165.

Berrisford, J.M., Baradaran, R., and Sazanov, L.A. (2016) Structure of bacterial respiratory complex I. *Biochim Biophys Acta* **1857**: 892–901.

Booth, I.R. (1985) Regulation of cytoplasmic pH in bacteria. *Microbiol Rev* **49**: 359–378.

Boucher, H.W., Talbot, G.H., Bradley, J.S., Edwards, J.E., Gilbert, D., Rice, L.B., *et al*. (2009) Bad bugs, no drugs: no ESKAPE! an update from the Infectious Diseases Society of America. *Clin Infect Dis* **48**: 1–12.

Boudker, O., Ryan, R.M., Yernool, D., Shimamoto, K., and Gouaux, E. (2007) Coupling substrate and ion binding to extracellular gate of a sodium-dependent aspartate transporter. *Nature* **445**: 387–393.

Chen, W. (2020) Host innate immune responses to *Acinetobacter baumannii* infection. *Front Cell Infect Microbiol* **10**: 486.

de Berardinis, V., Vallenet, D., Castelli, V., Besnard, M., Pinet, A., Cruaud, C., *et al*. (2008) A complete collection of single-gene deletion mutants of *Acinetobacter baylyi* ADP1. *Mol Syst Biol* **4**: 174.

Di Venanzio, G., Flores-Mireles, A.L., Calix, J.J., Haurat, M. F., Scott, N.E., Palmer, L.D., *et al*. (2019) Urinary tract colonization is enhanced by a plasmid that regulates uropathogenic *Acinetobacter baumannii* chromosomal genes. *Nat Commun* **10**: 1–13.

Dibrov, P., Dibrov, E., Pierce, G.N., and Galperin, M.Y. (2004) Salt in the wound: a possible role of Na^+ gradient in chlamydial infection. *Microbial Physiol* **8**: 1–6.

Dijkshoorn, L., Nemec, A., and Seifert, H. (2007) An increasing threat in hospitals: multidrug-resistant *Acinetobacter baumannii*. *Nat Rev Microbiol* **5**: 939–951.

Dimroth, P. (1980) A new sodium-transport system energized by the decarboxylation of oxaloacetate. *FEBS Lett* **122**: 234–236.

Falagas, M.E., and Karveli, E.A. (2007) The changing global epidemiology of *Acinetobacter baumannii* infections: a development with major public health implications. *Clin Microbiol Infect* **13**: 117–119.

Fang, H., Qin, X.-Y., Zhang, K.-D., Nie, Y., and Wu, X.-L. (2018) Role of the group 2 Mrp sodium/proton antiporter in rapid response to high alkaline shock in the alkaline- and salt-tolerant *Dietzia* sp. DQ12-45-1b. *Appl Microbiol Biotechnol* **102**: 3765–3777.

Farwick, M., Siewe, R.M., and Krämer, R. (1995) Glycine betaine uptake after hyperosmotic shift in *Corynebacterium glutamicum*. *J Bacteriol* **177**: 4690–4695.

Gebhardt, M.J., Gallagher, L.A., Jacobson, R.K., Usacheva, E.A., Peterson, L.R., Zurawski, D.V., and Shuman, H.A. (2015) Joint transcriptional control of virulence and resistance to antibiotic and environmental stress in *Acinetobacter baumannii*. *mBio* **6**: e01660-01615.

Godeux, A.-S., Svedholm, E., Lupo, A., Haenni, M., Venner, S., Laaberki, M.-H., and Charpentier, X. (2020) Scarless removal of large resistance Island AbaR results in antibiotic susceptibility and increased natural transformability in *Acinetobacter baumannii*. *Antimicrob Agents Chemother* **64**: e00951-00920.

Górecki, K., Hägerhäll, C., and Drakenberg, T. (2014) The Na^+ transport in Gram-positive bacteria defect in the Mrp antiporter complex measured with ^{23}Na nuclear magnetic resonance. *Anal Biochem* **445**: 80–86.

Green, E.R., Juttukonda, L.J., and Skaar, E.P. (2020) The manganese-responsive transcriptional regulator MumR protects *Acinetobacter baumannii* from oxidative stress. *Infect Immun* **88**: e00762-00719.

Grier, J.T., Arivett, B.A., Ramírez, M.S., Chosed, R.J., Bigner, J.A., Ohneck, E.J., *et al*. (2021) Two *Acinetobacter baumannii* isolates obtained from a fatal necrotizing fasciitis infection display distinct genomic and phenotypic characteristics in comparison to type strains. *Front Cell Infect Microbiol* **11**: 635673.

Hamamoto, T., Hashimoto, M., Hino, M., Kitada, M., Seto, Y., Kudo, T., and Horikoshi, K. (1994) Characteriza-

tion of a gene responsible for the Na^+/H^+ antiporter system of alkalophilic *Bacillus* species strain C-125. *Mol Microbiol* **14**: 939–946.

Harding, C.M., Hennon, S.W., and Feldman, M.F. (2018) Uncovering the mechanisms of *Acinetobacter baumannii* virulence. *Nat Rev Microbiol* **16**: 91–102.

Heise, R., Müller, V., and Gottschalk, G. (1992) Presence of a sodium-translocating ATPase in membrane vesicles of the homoacetogenic bacterium *Acetobacterium woodii*. *Eur J Biochem* **206**: 553–557.

Hesse, L.E., Lonergan, Z.R., Beavers, W.N., Skaar, E.P., and Whiteley, M. (2019) The *Acinetobacter baumannii* Znu system overcomes host-imposed nutrient zinc limitation. *Infect Immun* **87**: e00746-00719.

Hood, M.I., Mortensen, B.L., Moore, J.L., Zhang, Y., Kehl-Fie, T.E., Sugitani, N., *et al*. (2012) Identification of an *Acinetobacter baumannii* zinc acquisition system that facilitates resistance to calprotectin-mediated zinc sequestration. *PLoS Pathog* **8**: e1003068.

Hubloher, J.J., Schabacker, K., Müller, V., and Averhoff, B. (2021) CsrA coordinates compatible solute synthesis in *Acinetobacter baumannii* and facilitates growth in human urine. *Microbiol Spectr* **9**: e0129621.

Hubloher, J.J., Zeidler, S., Lamosa, P., Santos, H., Averhoff, B., and Müller, V. (2020) Trehalose-6-phosphate-mediated phenotypic change in *Acinetobacter baumannii*. *Environ Microbiol* **22**: 5156–5166.

Inaba, K., Kuroda, T., Shimamoto, T., Kayahara, T., Tsuda, M., and Tsuchiya, T. (1994) Lithium toxicity and $Na^+(Li^+)/H^+$ antiporter in *Escherichia coli*. *Biol Pharm Bull* **17**: 395–398.

Ito, M., Guffanti, A.A., Oudega, B., and Krulwich, T.A. (1999) *mrp*, a multigene, multifunctional locus in *Bacillus subtilis* with roles in resistance to cholate and to Na^+ and in pH homeostasis. *J Bacteriol* **181**: 2394–2402.

Ito, M., Guffanti, A.A., Wang, W., and Krulwich, T.A. (2000) Effects of nonpolar mutations in each of the seven *Bacillus subtilis mrp* genes suggest complex interactions among the gene products in support of Na^+ and alkali but not cholate resistance. *J Bacteriol* **182**: 5663–5670.

Ito, M., Morino, M., and Krulwich, T.A. (2017) Mrp antiporters have important roles in diverse bacteria and archaea. *Front Microbiol* **8**: 2325.

Jacobs, A.C., Thompson, M.G., Black, C.C., Kessler, J.L., Clark, L.P., McQueary, C.N., *et al*. (2014) AB5075, a highly virulent isolate of Acinetobacter baumannii, as a model strain for the evaluation of pathogenesis and antimicrobial treatments. *mBio* **5**: e01076-01014.

König, P., Averhoff, B., and Müller, V. (2021) K^+ and its role in virulence of *Acinetobacter baumannii*. *Int J Med Microbiol* **311**: 151516.

Kosono, S., Haga, K., Tomizawa, R., Kajiyama, Y., Hatano, K., Takeda, S., *et al*. (2005) Characterization of a multigene-encoded sodium/hydrogen antiporter (Sha) from *Pseudomonas aeruginosa*: its involvement in pathogenesis. *J Bacteriol* **187**: 5242–5248.

Kosono, S., Morotomi, S., Kitada, M., and Kudo, T. (1999) Analyses of a *Bacillus subtilis* homologue of the Na^+/H^+ antiporter gene which is important for pH homeostasis of alkaliphilic *Bacillus* sp. C-125. *Biochim Biophys Acta* **1409**: 171–175.

Kremp, F., and Müller, V. (2020) Methanol and methyl group conversion in acetogenic bacteria: biochemistry, physiology and application. *FEMS Microbiol Rev* **45**: fuaa040.

Krulwich, T.A., Hicks, D.B., and Ito, M. (2009) Cation/proton antiporter complements of bacteria: why so large and diverse? *Mol Microbiol* **74**: 257–260.

Krulwich, T.A., Sachs, G., and Padan, E. (2011) Molecular aspects of bacterial pH sensing and homeostasis. *Nat Rev Microbiol* **9**: 330–343.

Lee, J.C., Koerten, H., van den Broek, P., Beekhuizen, H., Wolterbeek, R., van den Barselaar, M., *et al*. (2006) Adherence of *Acinetobacter baumannii* strains to human bronchial epithelial cells. *Res Microbiol* **157**: 360–366.

Lucidi, M., Runci, F., Rampioni, G., Frangipani, E., Leoni, L., and Visca, P. (2018) New shuttle vectors for gene cloning and expression in multidrug-resistant *Acinetobacter* species. *Antimicrob Agents Chemother* **62**: e02480-02417.

McConnell, M.J., Actis, L., and Pachón, J. (2013) *Acinetobacter baumannii*: human infections, factors contributing to pathogenesis and animal models. *FEMS Microbiol Rev* **37**: 130–155.

McKee, M., Exall, S., Stuckler, D., and Wolff, A. (2016) 'Normal' serum sodium concentration among inpatients over 65 admitted to hospital: an observational study. *Postgrad Med J* **92**: 21–26.

Mitchell, P. (1961) Coupling of phosphorylation to electron and hydrogen transfer by a chemi-osmotic type of mechanism. *Nature* **191**: 144–148.

Morris, F.C., Dexter, C., Kostoulias, X., Uddin, M.I., and Peleg, A.Y. (2019) The mechanisms of disease caused by *Acinetobacter baumannii*. *Front Microbiol* **10**: 1601.

Mortensen, B.L., and Skaar, E.P. (2013) The contribution of nutrient metal acquisition and metabolism to *Acinetobacter baumannii* survival within the host. *Front Cell Infect Microbiol* **3**: 95.

Müller, V., and Bowien, S. (1995) Differential effects of sodium ions on motility in the homoacetogenic bacteria *Acetobacterium woodii* and *Sporomusa sphaeroides*. *Arch Microbiol* **164**: 363–369.

Müller, V., and Gottschalk, G. (1992) Na^+ translocation in the course of methanogenesis from methanol or formaldehyde. In *Alkali Cation Transport Systems in Procaryotes*, Bakker, E.P. (ed). Boca Raton, USA: CRC Press, pp. 155–178.

Müller, V., and Hess, V. (2017) The minimum biological energy quantum. *Front Microbiol* **8**: 2019.

Murin, C.D., Segal, K., Bryksin, A., and Matsumura, I. (2012) Expression vectors for *Acinetobacter baylyi* ADP1. *Appl Environ Microbiol* **78**: 280–283.

Padan, E., Bibi, E., Ito, M., and Krulwich, T.A. (2005) Alkaline pH homeostasis in bacteria: new insights. *Biochim Biophys Acta Biomembr* **1717**: 67–88.

Padan, E., and Schuldiner, S. (1993) Na^+/H^+ antiporters, molecular devices that couple the Na^+ and H^+ circulation in cells. *J Bioenerg Biomembr* **25**: 647–669.

Padan, E., and Schuldiner, S. (1994) Molecular physiology of Na^+/H^+ antiporters, key transporters in circulation of Na^+ and H^+ in cells. *Biochim Biophys Acta* **1185**: 129–151.

Peleg, A.Y., de Breij, A., Adams, M.D., Cerqueira, G.M., Mocali, S., Galardini, M., *et al*. (2012) The success of

Acinetobacter species; genetic, metabolic and virulence attributes. *PLoS One* **7**: e46984.

Perez, C., Faust, B., Mehdipour, A.R., Francesconi, K.A., Forrest, L.R., and Ziegler, C. (2014) Substrate-bound outward-open state of the betaine transporter BetP provides insights into Na^+ coupling. *Nat Commun* **5**: 4231.

Plough, I.C., and Baker, E.M. (1959) Maximum physiological concentration of sodium in human urine. *J Appl Physiol* **14**: 1036–1038.

Poirel, L., Menuteau, O., Agoli, N., Cattoen, C., and Nordmann, P. (2003) Outbreak of extended-spectrum beta-lactamase VEB-1-producing isolates of *Acinetobacter baumannii* in a french hospital. *J Clin Microbiol* **41**: 3542–3547.

Rimon, A., Tzubery, T., and Padan, E. (2007) Monomers of the NhaA Na^+/H^+ antiporter of *Escherichia coli* are fully functional yet dimers are beneficial under extreme stress conditions at alkaline pH in the presence of Na^+ or Li^+. *J Biol Chem* **282**: 26810–26821.

Runci, F., Gentile, V., Frangipani, E., Rampioni, G., Leoni, L., Lucidi, M., *et al*. (2019) Contribution of active iron uptake to *Acinetobacter baumannii* pathogenicity. *Infect Immun* **87**: e00755-00718.

Samir, R., Hussein, S.H., Elhosseiny, N.M., Khattab, M.S., Shawky, A.E., and Attia, A.S. (2016) Adaptation to potassium-limitation is essential for *Acinetobacter baumannii* pneumonia pathogenesis. *J Infect Dis* **214**: 2006–2013.

Schmidt, K., Liaaen-Jensen, S., and Schlegel, H.G. (1963) Die Carotinoide der *Thiorhodaceae*. I. Okenon als Hauptcarotenoid von *Chromatium okenii perty*. *Arch Microbiol* **46**: 117–126.

Schubiger, C.B., Hoang, K.H.T., and Häse, C.C. (2020) Sodium antiporters of *Pseudomonas aeruginosa* in challenging conditions: effects on growth, biofilm formation, and swarming motility. *J Genet Eng Biotechnol* **18**: 4.

Schuchmann, K., and Müller, V. (2014) Autotrophy at the thermodynamic limit of life: a model for energy conservation in acetogenic bacteria. *Nat Rev Microbiol* **12**: 809–821.

Sheldon, J.R., and Skaar, E.P. (2020) *Acinetobacter baumannii* can use multiple siderophores for iron acquisition, but only acinetobactin is required for virulence. *PLoS Pathog* **16**: e1008995.

Skulachev, V.P. (1989) The sodium cycle: a novel type of bacterial energetics. *J Bioenerg Biomembr* **21**: 635–647.

Skulachev, V.P. (1991) Chemiosmotic systems in bioenergetics: H^+-cycles and Na^+-cycles. *Biosci Rep* **11**: 387–441.

Stahl, J., Bergmann, H., Göttig, S., Ebersberger, I., and Averhoff, B. (2015) *Acinetobacter baumannii* virulence is mediated by the concerted action of three phospholipases D. *PLoS One* **10**: e0138360.

Steiner, J., and Sazanov, L. (2020) Structure and mechanism of the Mrp complex, an ancient cation/proton antiporter. *eLife* **9**: e59407.

Steuber, J., Halang, P., Vorburger, T., Steffen, W., Vohl, G., and Fritz, G. (2014) Central role of the Na^+-translocating NADH:quinone oxidoreductase (Na^+-NQR) in sodium bioenergetics of *Vibrio cholerae*. *Biol Chem* **395**: 1389–1399.

Talyansky, Y., Nielsen, T.B., Yan, J., Carlino-Macdonald, U., Di Venanzio, G., Chakravorty, S., *et al*. (2021) Capsule carbohydrate structure determines virulence in *Acinetobacter baumannii*. *PLoS Pathog* **17**: e1009291.

Tucker, A.T., Nowicki, E.M., Boll, J.M., Knauf, G.A., Burdis, N.C., Trent, M.S., and Davies, B.W. (2014) Defining gene-phenotype relationships in *Acinetobacter baumannii* through one-step chromosomal gene inactivation. *mBio* **5**: e01313-01314.

Vaish, M., Price-Whelan, A., Reyes-Robles, T., Liu, J., Jereen, A., Christie, S., *et al*. (2018) Roles of *Staphylococcus aureus* Mnh1 and Mnh2 antiporters in salt tolerance, alkali tolerance, and pathogenesis. *J Bacteriol* **200**: e00611-00617.

Wang, C.-Y., Cogswell, M.E., Loria, C.M., Chen, T.-C., Pfeiffer, C.M., Swanson, C.A., *et al*. (2013) Urinary excretion of sodium, potassium, and chloride, but not iodine, varies by timing of collection in a 24-hour calibration study. *J Nutr* **143**: 1276–1282.

Weidensdorfer, M., Ishikawa, M., Hori, K., Linke, D., Djahanschiri, B., Iruegas, R., *et al*. (2019) The *Acinetobacter* trimeric autotransporter adhesin Ata controls key virulence traits of *Acinetobacter baumannii*. *Virulence* **10**: 68–81.

Wilson, T.H., and Ding, P.Z. (2001) Sodium-substrate cotransport in bacteria. *Biochim Biophys Acta* **1505**: 121–130.

World Health Organization. (2017) Global priority list of antibiotic-resistant bacteria to guide research, discovery, and development of new antibiotics. https://www.who.int/news/item/27-02-2017-who-publishes-list-of-bacteria-for-which-new-antibiotics-are-urgently-needed

eidler, S., Hubloher, J., Schabacker, K., Lamosa, P., Santos, H., and Müller, V. (2017) Trehalose, a temperature- and salt-induced solute with implications in pathobiology of *Acinetobacter baumannii*. *Environ Microbiol* **19**: 5088–5099.

Zeidler, S., and Müller, V. (2019a) Coping with low water activities and osmotic stress in *Acinetobacter baumannii*: significance, current status and perspectives. *Environ Microbiol* **21**: 2212–2230.

Zeidler, S., and Müller, V. (2019b) The role of compatible solutes in desiccation resistance of *Acinetobacter baumannii*. *Microbiology* **8**: e00740.

Supporting Information

Additional Supporting Information may be found in the online version of this article at the publisher's web-site:

Appendix S1. Supporting Information.